

# Supporting Information

## Trembath-Reichert et al. 10.1073/pnas.1707525114

### Geochemical Analyses

DIC samples were injected into preweighed, He-flushed Exetainer vials (Labco Limited) containing 100  $\mu\text{L}$  of 40% phosphoric acid. Concentrations and stable carbon isotopes of DIC were measured on a Gasbench II (Thermo Scientific) coupled to a Delta V Plus IRMS instrument (Thermo Scientific) in the Caltech Stable Isotope Facility, following the methods of Torres et al. (72). Briefly, Exetainers were sampled using a Gas Chromatograph Prep and Load autosampler (CTC Analytics) equipped with a doubled-holed needle that transferred headspace using a  $0.5 \text{ mL} \cdot \text{min}^{-1}$  continuous flow of He to a  $50\text{-}\mu\text{m}$  sample loop before separation by a PoraPlotQ fused silica column (25 m, i.d. =  $0.32 \text{ mm}$ ) at  $72^\circ\text{C}$ . A  $20 \text{ mM}$   $\text{NaHCO}_3$  solution was used to establish a DIC concentration standard curve by comparing the average of the total peak area (masses 44, 45, and 46) of replicate sample injections with the volume of  $\text{NaHCO}_3$  added. Using the estimated error in the volume measurement and the SD of the peak area for the total carbon of bicarbonate standards, the estimated error of DIC concentrations was  $\pm 0.009 \mu\text{mol}$ . The  $\delta^{13}\text{C}$  values were corrected for sample size dependency and then normalized to the Vienna Pee Dee Belemnite scale with a three-point correction (73) using National Bureau of Standards standard 19, a previously calibrated internal laboratory standard, and the average of all of the  $\text{NaHCO}_3$  standards. Accuracy ( $0.11\%$ ,  $n = 79$ ) was determined by considering independent standards as samples, and precision ( $0.5\%$ ) was determined from replicate measurements of all standard solutions.

Methane headspace concentrations were measured relative to argon (added to *ca.* equal partial pressure in all incubations) using a Hewlett Packard 5972 Series Mass Selective Detector and Hewlett Packard 5890 Series II Plus Gas Chromatograph at the Caltech Environmental Analysis Center. The  $\delta^{13}\text{C}\text{-CH}_4$  was analyzed as per the methods of Tsunogai et al. (74), and  $\delta^2\text{H}\text{-CH}_4$  was analyzed as per the methods of Kikuchi et al. (75) at the Kochi Institute for Core Sample Research, Japan Agency for Marine-Earth Science and Technology (JAMSTEC).

### Isotope Calculations

Isotope mass balance was calculated using Eqs. S1 and S2, where  $n$  is the number of moles,  $F$  is the fractional abundance of the rare isotope (Eq. S3), and  $R$  is the ratio of ion counts of the rare isotope over ion counts of the more abundant isotope (76).  $F_{\text{total}}$ ,  $n_{\text{total}}$ ,  $F_{\text{substrate}}$ , and  $F_{\text{background}}$  were known and used to solve for  $n_{\text{substrate}}$ . Fractional abundances are displayed as atom percent, which is 100-fold the fractional abundance (Eq. S4). DIC production rates were calculated by dividing the moles of DIC from substrate ( $n_{\text{substrate}}$ ) by sample volume ( $4 \text{ cm}^3$  for coal samples) and days of incubation (864 d). The percent molar methane from substrate was calculated from Eq. S5, a rearrangement of Eqs. S1 and S2:

$$n_{\text{total}} = n_{\text{substrate}} + n_{\text{background}}, \quad [\text{S1}]$$

$$n_{\text{total}} \times F_{\text{total}} = n_{\text{substrate}} \times F_{\text{substrate}} + n_{\text{background}} \times F_{\text{background}}, \quad [\text{S2}]$$

$$F = \frac{R}{1+R}, \quad [\text{S3}]$$

$$\text{At. \%} = F \times 100, \quad [\text{S4}]$$

$$\begin{aligned} & (F_{\text{total}} - F_{\text{background}}) / (F_{\text{substrate}} - F_{\text{background}}) \\ & = (n_{\text{substrate}} / n_{\text{total}}) \times 100. \end{aligned} \quad [\text{S5}]$$

Data analysis and display as violin plots of the kernel density function were done using R (77) with the “ggplot2” (78), “dplyr” (79), “gridExtra” (80), and “RColorBrewer” (81) packages. Cell ROIs with deuterium enrichment at least 10-fold above natural abundance were deemed “active.” This threshold was chosen as a number that was sufficiently higher than natural abundance to account for remnant isotope from hydrogen exchange and error in the NanoSIMS measurement. Our chosen threshold ( $0.115 \text{ at. \%}$ ) is about half of that used by Kopf et al. (22) and a third of that reported by Berry et al. (21) for deuterium background in fixed pure culture studies.

For generation time calculations, a conservative approach was used that only included ROIs where  $^{15}\text{N}^{12}\text{C}$  counts were above the Poisson error provided by Look@NanoSIMS. Poisson error is based on the theoretical precision of the mean for the minor ion. Eqs. S6 and S7 were used to calculate the rate of biomass generation via fractional abundance of isotope label in cellular biomass over the incubation period, where  $\mu$  is the generation rate (encompassing both cell maintenance and generation of new cells),  $T_{\text{final}}$  is the length of the incubation,  $F_{\text{label}}$  is the labeling strength,  $F_{\text{final}}$  is the single-cell NanoSIMS measurement, and  $F_{\text{nat}}$  is the natural abundance. We used Eq. S8 to estimate generation time, as the reciprocal of the rate, per Zilversmit et al. (82). NanoSIMS  $^2F$  and  $^{15}F$  values were multiplied by a conversion factor determined for single-cell to bulk isotope measurements by Kopf et al. (22) of  $0.67$  ( $^2\text{H}$ ) and  $0.94$  ( $^{15}\text{N}$ ). While lipid water assimilation values are not known for this system, the maximal value ( $a_w$  of  $0.83$ ) from Zhang et al. (83) was used as an upper estimate of assimilation based on findings that lipid water assimilation increases as growth rate decreases (84). Nitrogen-based rate calculations assumed all nitrogen was derived from the substrate (methylamine or ammonium); therefore, the assimilation constant was excluded from Eq. S7:

$$^2\mu = \left( -\ln \left( 1 - \frac{(2F_{\text{final}} - 2F_{\text{nat}})}{a_w(2F_{\text{label}} - 2F_{\text{nat}})} \right) \right) / T_{\text{final}}, \quad [\text{S6}]$$

$$^{15}\mu = \left( -\ln \left( 1 - \frac{(15F_{\text{final}} - 15F_{\text{nat}})}{(15F_{\text{label}} - 15F_{\text{nat}})} \right) \right) / T_{\text{final}}, \quad [\text{S7}]$$

$$\tau = \mu^{-1}. \quad [\text{S8}]$$

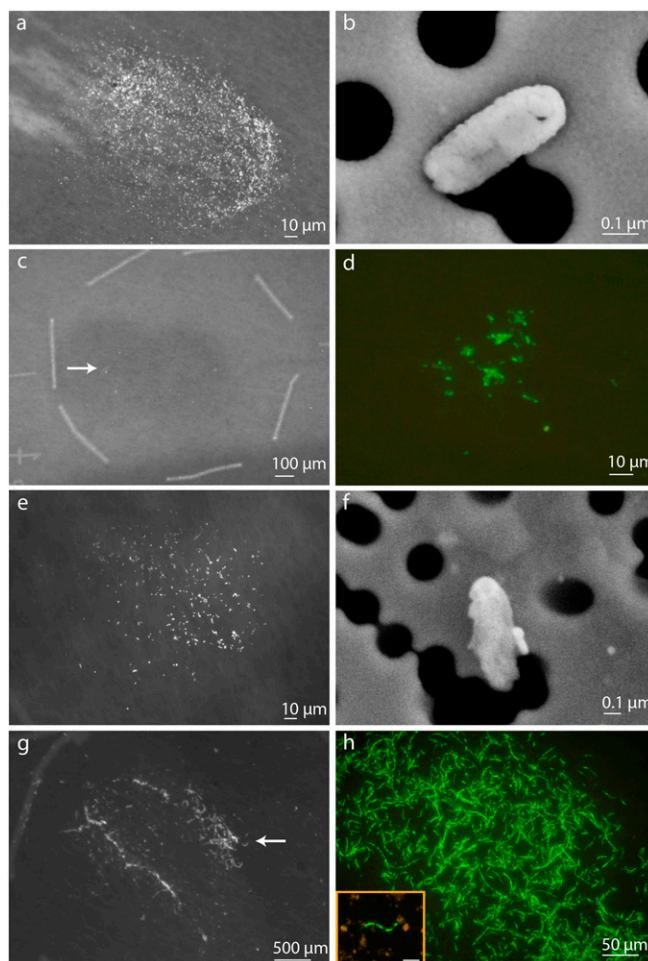


**Fig. S1.** SYBR-stained cells after separation and FACS concentration on ITO-coated 0.2- $\mu\text{m}$  polycarbonate NanoSIMS membranes from the two highest cell abundance conditions in 15R3 coal and mixed lithology. SYBR and SEM images highlight some distinctions in cell morphology between the two methanol amended samples. White arrows indicate region of SYBR image on larger membrane target area. The 15R3 coal incubation amended with methylamine (A), SEM image of A (B), 15R3 coal amended with methanol (C), C magnified with false color (D), mixed lithology amended with methanol +  $\text{H}_2$  + ammonium (E), SEM image of E (F), mixed lithology amended with methanol (G), and mixed lithology amended with methanol magnified with false color (H; Inset, the same sample filtered before cell sorting to demonstrate cell density without concentration). (Scale bar: H, Inset, 20  $\mu\text{m}$ .)

## Other Supporting Information Files

[Dataset S1 \(XLSX\)](#)

[Dataset S2 \(XLSX\)](#)